

# Testing the Efficiency of a Heat Pump with Radiant Systems in Heating Mode

Martin Šimko<sup>1\*</sup>, Dušan Petráš<sup>1</sup>, Daniel Szabó<sup>1</sup>, Lukáš Živner<sup>2</sup>, Ján Takács<sup>1</sup>

<sup>1</sup> Faculty of Civil Engineering, Slovak University of Technology in Bratislava, Radlinskeho 2766/11, 810 05 Bratislava, Slovakia

<sup>2</sup> NIBE, s. r. o., Dražice 69, 294 71 Benátky nad Jizerou, Czech Republic

\* Corresponding author, e-mail: [martin.simko@stuba.sk](mailto:martin.simko@stuba.sk)

Received: 06 March 2024, Accepted: 13 October 2024, Published online: 22 October 2024

## Abstract

The paper deals with the experimental testing of the efficiency of the operation of an air/water heat pump in connection with three radiant systems in heating mode in an office building, which is part of the central laboratories of the Slovak university of Technology in Bratislava. The testing was aimed at verifying the manufacturer's theoretical claims about efficiency of the heat pump based on the COP and SCOP values according to EN 14511-1:2022 and EN 14825:2022. The testing period was from 7 Jan. 2024 until 15 Jan. 2024. The aim of the testing measurements was to evaluate the calculated value of SPF efficiency for individual days and for the testing period. During the measuring period, the wall radiant system consumed 188 kWh, the ceiling system 216 kWh, and the floor radiant system 196 kWh. The heat pump consumed 227 kWh of electricity. The calculated SPF value was 2.64.

## Keywords

heat pump, low-temperature radiant systems, coefficient of performance (COP), seasonal performance factor (SPF)

## 1 Introduction

Nowadays, when energy prices are increasing and at the same time there is an emphasis on reducing dependence on the consumption of primary energy sources (e.g., natural gas), a heat pump (HP) can be a suitable alternative source of heating/cooling, using the energy of the surrounding environment as a renewable energy source (RES). Running large area radiant systems [1, 2] together with an air to water heat pump can lead to lower operating loads. Experimental measurements are based on the evaluation of the efficiency of heat pump operation together with low-temperature large area radiant systems in heating mode, the so-called seasonal performance factor (SPF) [3].

It has also been shown that it is important to consider the local climate when designing a HP, as it significantly affects its annual performance [4]. It is also important that the air-to-water heat pump is properly sized and operated to achieve high SPF [5, 6, 7, 8, 9].

The present experimental measurement was focused on testing the efficiency of the heat pump in cooperation with low temperature large area radiant systems in heating mode [10, 11]. Three separate rooms were used, where the first room had floor heating, the second room had ceiling

heating and the third room had wall heating. These three rooms are located in a real office building. The three rooms are used as a laboratory setting for the investigation of radiant heating systems utilising the air source HP.

The systems in all rooms are based on the so-called dry system, where the radiating surface of the radiant floor system consists of boards and in the case of ceiling and wall radiant systems of plasterboard boards. Each system had its own heat meter installed at the manifolds of each system. The data acquisition, heat pump control and electrical distribution sub-cabinet were installed in a separate technical room. A 6 kW air/water HP was selected and installed on the roof of the building, approximately 5 m from the technical room. In order to measure the electricity consumption, the heat pump was connected to a certified impulse electricity meter of the type LE-01d MID. For the measurement period, the automatic control mode of the heat pump was selected, which uses the equithermal curve to calculate the required flow temperature of the heat-carrying medium.

It should be noted that the building in which the measurements were carried out was not insulated and there

was no active heating in the surrounding indoor spaces, and the air temperature in these spaces was around 7 to 9 °C during the period in question, which increases the demands on the performance of large area radiant systems.

## 2 Basis of heat pumps and SPF

The heat pump principle works according to the Carnot cycle (Fig. 1). HP converts environmental energy and electricity directly into heat, which can be led into heated spaces. In winter, it transfers heat from the outside to the inside to heat the occupied space, and in summer it removes heat in the opposite direction from the occupied space to the heat source (Fig. 2) [12, 13, 14].

The utilization of HP in conjunction with radiant floor, wall and ceiling heating systems, can facilitate enhancements to the low exergy system. Heat transfer is a process whereby heat is transferred from one location to another.

The utilization of a heat pump as a heat source in conjunction with an integrated radiant heating system within the designated heating room, operating at a temperature of the heat carrier liquid in close proximity to the operating room air temperature, has been demonstrated to be

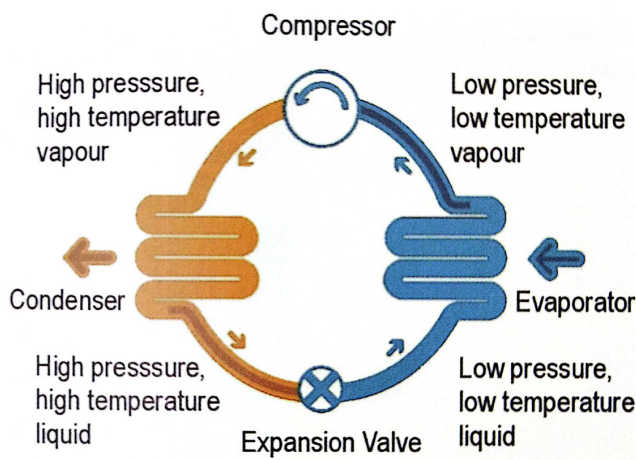


Fig. 1 HP and Carnot cycle [12]

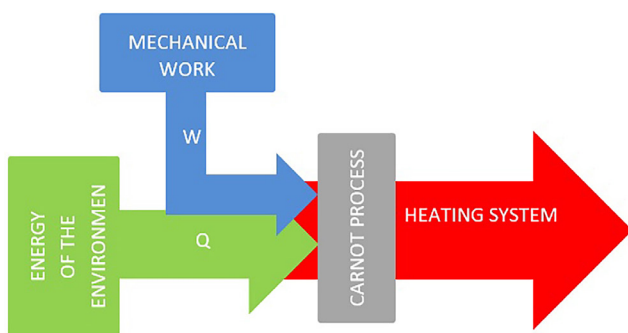


Fig. 2 Working principle of heat pump [12]

an extremely effective approach. The HP will have a high coefficient of performance (COP), which expresses the energy efficiency of the HP for heating, i.e., the ratio of heat output to energy input (electricity) (Fig. 2) [12, 13, 14].

A HP can be defined as a low-temperature heat source (energy from the environment) that converts low-temperature heat into high-temperature heat and heat consumed by the heat consumer (Fig. 3) [15].

HP can be classified according to the way they extract energy from the environment (Heat Source):

Ground source HP (GSHP) using the heat of the ground through ground collectors or boreholes – ground/water type, water source HP (WSHP) using the heat of the underground water or collector in the lake – water/water type, air source HP (ASHP) using the air which is ventilated to the heat exchanger of the HP or using ventilation pipes (ventilation HP) – air/water type and the HP using the return pipe of the district heating as the heat source of the HP [15].

One of the study aims to analyze the performance of the WSHP, GSHP and ASHP systems for large office buildings using a dynamic energy simulation. The SPF of the system was calculated as 3.8 and 2.5 for a WSHP system, 3.8 and 2.6 for a GSHP system, and 2.9 and 1.7 for an ASHP system during the cooling and heating periods, respectively [16]. Similar research has also focused on experimental exergetic comparisons of different types of HP: as air to air, air to water, water to water and water to air [17].

ASHP are part of the solution to decarbonise the residential heating sector. The COP is a measure of the instantaneous efficiency of a HP. The heat energy produced by an ASHP is deemed renewable if it meets a specified sustained COP over a period of time, e.g., a SPF [18].

Air-to-water HP are regarded as a fundamental part of many proposed climate action plans in heating dominated climates. However, individual studies have concluded that this technology generally underperforms in practice when compared to its rated performance. Of the 378 HP reviewed, it was found that the average SPF was 2.59, significantly lower than typical product rated performances.

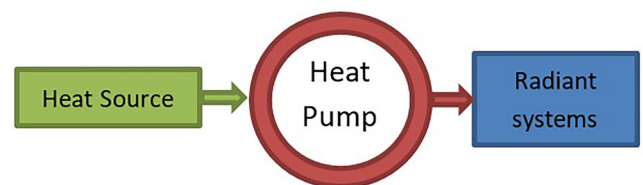


Fig. 3 System theory scheme of the heat pump system [15]

Three reasons for this underperformance include, misrepresentative weather data for certain locations, unaccounted for losses in the distribution pipes and unaccounted for effects of cycling [19].

### 3 Tested heat pump

Tested HP was ASHP. The ASHP represented model F2040-6, controlled by an inverter, was designed for experimental measurements in conjunction with radiant systems. The operating range of the HP is from  $-20$  to  $43$  °C, with a maximum exterior temperature of the heat transfer medium of  $58$  °C. In addition to heating, the HP can also be used for cooling during summer months through reverse operation. Fig. 4 displays a boiler-type F2040-6 ASHP including its individual components: evaporator, compressor and condenser.

Fig. 5 provides a detailed schematic of the ASHP external module F2040-6, which elucidates the interconnection of the components depicted in Fig. 4 with greater precision.

Fig. 5 displays the diagram of the ASHP type F2040-6 external module, which includes individual sensors – such as the external air temperature sensor, the temperature sensor on the compressor discharge, the temperature sensor on the evaporator, the temperature sensor of the supply temperature of the heat-carrying working substance behind the condenser, the temperature sensor on the return pipe, the temperature sensor behind condenser, high-pressure sensor.

The technical specifications of the tested ASHP type F2040/6 are listed in Table 1, including performance range, operating voltage, maximum cooling capacity, etc.

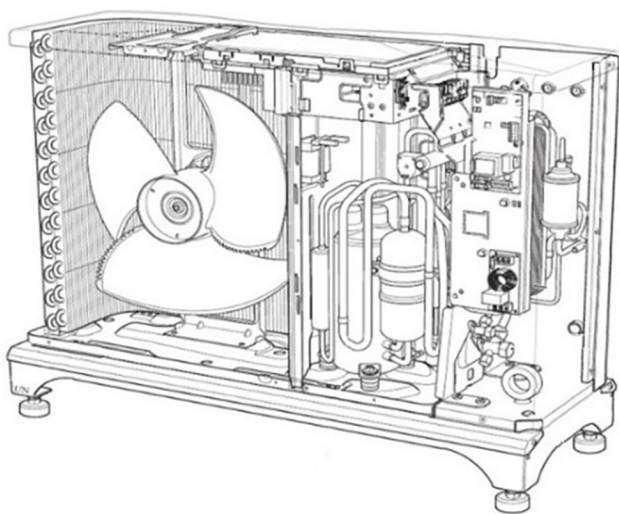


Fig. 4 ASHP type F2040-6 [20]

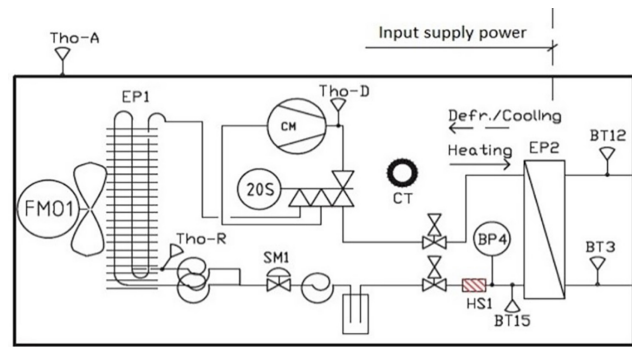


Fig. 5 Scheme of external module F2040-6 [20] Explanations: **BT 28 (Tho-A)** – external air temperature sensor, **BT 14 (Tho-D)** – compressor discharge temperature sensor, **BT 16 (Tho-R)** – temperature sensor on the evaporator, **BT 12** – temperature sensor of the supply temperature of the heat-carrying working substance behind the condenser, **BT 3** – temperature sensor of the heat-carrying working substance on the return pipe, **BT 15** – temperature sensor behind the condenser, **BP 4** – high pressure sensor, **CM** – compressor, **EP 2** – Condenser, **EP 1** – Evaporator, **QN 3 (SM1)** – expansion valve, **QN 2 (20S)** – four-way valve, **HS 1** – filter dehydrator [20]

Table 1 Technical specifications of the ASHP type F2040-6 [20, 21]

Technical parameter	Specification
Power range A7/W35 [kW] (EN 14511-1:2022)	1.5 – 7
Power range A7/W45 [kW] (EN 14511-1:2022)	1.2 – 4.6
SCOP average climate zone 35/55 °C (EN 14825:2022)	4.8 / 3.46
Max. cooling capacity at A27/W7 [kW]	5.87
Max. cooling capacity at A27/W18 [kW]	7.98
Max. cooling capacity at A35/W7 [kW]	4.86
Max. cooling capacity at A35/W18 [kW]	7.03
Operating voltage	230 V / 50 Hz
Compressor	Double rotary

### 4 Experimental measurement of heat pump operation with large area radiant systems in heating mode

The experimental measurement took place in the laboratory conditions of the STU Faculty of Civil Engineering in Bratislava. The measurement took place in the period from 7.1.2024 to 15.1.2024. The subject of the experimental measurement was to investigate the efficiency of the heat pump with low-temperature large-area radiant systems in the heating mode. Electricity consumption by the heat pump was measured by a pulsed electricity meter LE-01d MID (EM – electric meter on Fig. 6).

The consumed heat was individually measured for each low-temperature large-area radiant system separately by ultrasonic heat meters T330 (HM1, HM2 and HM3 on Fig. 6). The temperature of the exterior air was also measured by a temperature sensor located on the heat pump

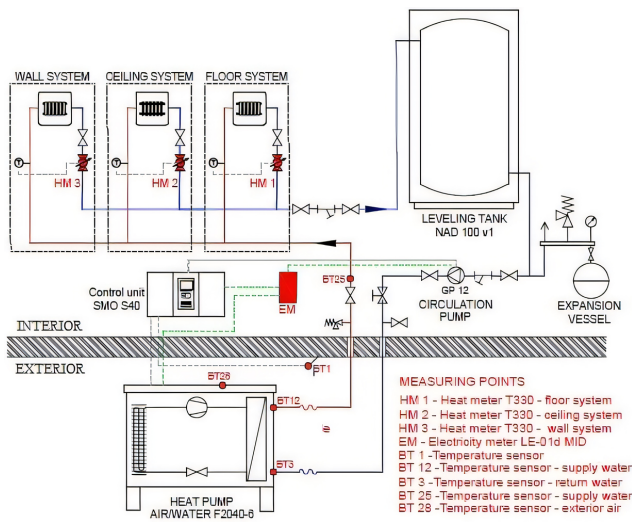


Fig. 6 Scheme of measuring points

(Tho-A on Fig. 4 and BT 28 on Fig. 5). Subsequently, the SPF value, which deals with the efficiency of the heat pump, was calculated. This calculated value was compared with the COP value given by the manufacturer.

#### 4.1 Radiant heating systems with tested ASHP

The study measured the thermal energy consumption of radiant systems (floor, ceiling and wall) connected to the ASHP in heating mode. The systems were designed for separate rooms with the same layout and floor area, all facing east. The Siccus dry large-area radiant floor system was installed in the first office room using two circuits with a pipe spacing of 150 mm, with Comfort Pipe PLUS pipes  $\Phi 14 \times 2.0$  mm, covering a radiant area of 15 m<sup>2</sup>. In the second room, the large-area dry radiant ceiling system was installed with PE-Xa pipe  $\Phi 9.9 \times 1.1$  mm with 8 panels 2000  $\times$  625 mm with a radiant area of 10 m<sup>2</sup>. In the third room features a large wall radiant system, which includes an PE-Xa pipe  $\Phi 9.9 \times 1.1$  mm and with 8 panels 2000  $\times$  625 mm a radiant surface of 10 m<sup>2</sup>.

#### 4.2 Water temperature in supply and return pipes and exterior temperature

The experiment began on 7 Jan. 2024 at the midnight. The SMO S40 heat pump control unit was used to set equithermal curve number 5. This curve required the heat pump to maintain a temperature of 38 °C in the heat-carrying working substance supply pipe, despite an outside temperature of – 11 °C. The initial design temperature drop was 38/33 °C (Fig. 7). On Wednesday 10.1.2024 at 9:00 a.m. was used to set equithermal curve number 7. This curve required the heat pump to maintain a temperature of

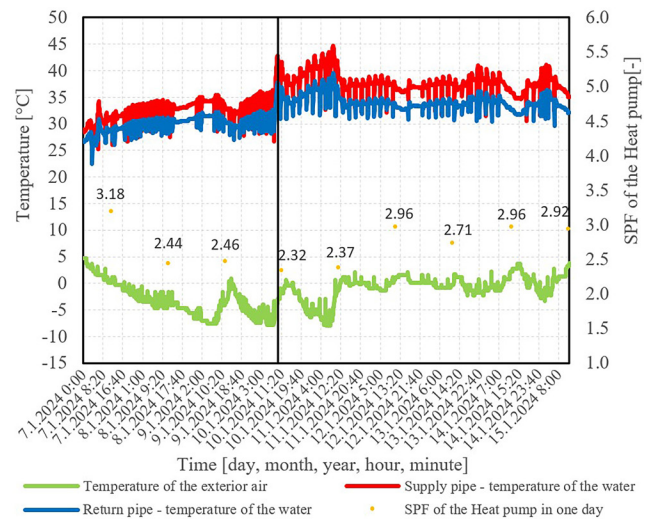


Fig. 7 Temperature of the water in the supply and return pipes, temperature of the exterior air and SPF of the ASHP

45 °C in the heat-carrying working substance supply pipe, despite an outside temperature of – 11 °C. The initial design temperature drop was 45/40 °C (Fig. 7).

Fig. 7 shows the exterior temperature on the primary axis graph. The average temperature of the exterior air during the measured period from 7 Jan. to 15 Jan. 2024 was –1.79 °C. Additionally, the temperature of the heat-carrying working substance in the supply and return pipes is also displayed on the same graph on the primary axis. It can be seen that the equithermal regulation reliably responded to the change of the outside temperature. When the temperature of the exterior air dropped, the heat pump in cooperation with the SMO S40 control unit, increased the temperature of the heat-carrying working substance in the supply pipe. Conversely, when the temperature of the exterior air increase, it lowered the temperature of the heat-carrying working substance in the supply pipe (Fig. 7).

Fig. 7 shows a graph divided by a vertical line, separating the period from 7 Jan. 2024 at the midnight to 10 Jan. 2024 9:00, when the equithermal curve number 5. was set in the control unit SMO S40 of heat pump. The average temperature of the heat-carrying substance was 32.56 °C.

During the period from 10 Jan. 2024 at 9:00 a.m. to 15 Jan. 2024 at 12:30 p.m., the equithermal curve was set to Number 7. The average temperature of the heat-carrying working substance was 37.77 °C. Throughout the measured period from 7 Jan. 2024 to 15 Jan. 2024 the average temperature of the heat-carrying substance was 35.71 °C. Fig. 7 shows the calculated values of the SPF of the ASHP displayed on the secondary axis. The values of the SPF of the ASHP represented the values calculated



from measured values of the thermal energy consumptions of the three radiant systems and measured electricity consumption of the ASHP of the individually day. The values of the SPF of the ASHP were higher when the values of the exterior air temperature were positive and decreased as the values of the exterior air temperature reached negative values.

### 4.3 Electricity consumption by ASHP and thermal energy consumption by radiant systems in heating mode

Fig. 8 displays the graphical outputs of the values of the thermal energy consumption and electricity consumption. Fig. 8 shows the thermal energy consumption of three low-temperature large-area radiant systems (radiant floor, ceiling, wall) on the primary axis. The blue curve represents the thermal energy consumption of the wall radiant system, the orange curve represents the thermal energy consumption of the ceiling radiant system and the gray curve represents the thermal energy consumption of the radiant floor system. Fig. 8 also shows the electric consumption with red curve of the ASHP on the secondary axis of the graph. During the entire measured period from 7 Jan. 2024 to 15 Jan. 2024, the radiant wall system consumed 188 kWh of the thermal energy, the ceiling radiant system 216 kWh and the floor radiant system 196 kWh, together with the low-temperature large-area radiant systems consumed 607 kWh of thermal energy. The ASHP consumed 227 kWh of the electricity energy during the same measured period (Fig. 8).

The electricity consumption curve became steeper as the exterior air temperature dropped due to the equithermal regulation of the heat-carrying working substance in the supply pipe. The ASHP took part in the electric consumption together with other circulation devices. Additionally, a change in the equithermal curve setting from no. 5 to

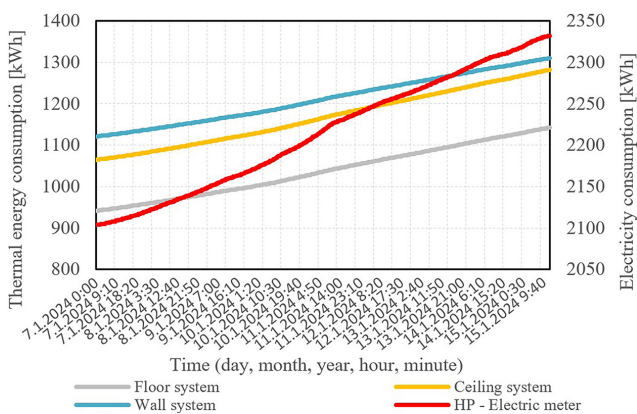


Fig. 8 Thermal energy consumption of low-temperature large-area radiant systems in heating mode and the electric consumption by the ASHP

no. 7 in 10 Jan. 2024 at 9:00 a.m., this resulted to change of the electricity consumption curve too.

Table 2 displays the values of the thermal energy consumption by the radiant systems and electric consumption by the ASHP for individually days of the measured period.

### 4.4 Calculation of the SPF and COP of the ASHP

To evaluation of the HP efficiency, we needed data on both the thermal energy consumed by the three large-area radiant systems and the electrical energy consumed by the ASHP. The SPF is the ratio of the heat supplied by the HP during the entire year of operation to the total energy consumed by the compressor and other circulation devices [22, 23]. SPF was calculated as follows:

$$SPF = \frac{\sum \Phi_K}{\sum P_K}, \tag{1}$$

where  $\Phi_K$  is the sum of the heat produced by the heat pump (kWh) and  $P_K$  is sum of thermal energy consumed by the compressor and other circulation devices (kWh) [22, 23].

The energy efficiency of systems working on the basis of thermodynamic cooling circulation (cooling and air conditioning equipment and HPs) evaluated by the so-called performance number COP, it is possible to express for the compressor heat pump as follows [22, 24]:

$$COP_{HP} = \frac{\Phi_K}{P_K}, \tag{2}$$

where  $\Phi_K$  is the heat produced by the heat pump (kWh) and  $P_K$  is thermal energy consumed by the compressor and other circulation devices (kWh) [22, 24].

The manufacturer provides the COP value, which can be found at the intersection of the exterior air and the curve representing the temperature of the heat-carrying working substance in the supply pipe (Fig. 9). The average outdoor air temperature during the measure period from 7 Jan. 2024 to 15 Jan. 2024 was  $-1.79\text{ }^\circ\text{C}$  [20].

The average temperature of the heat-carrying working substance during the measured period from 7 Jan. 2024 to 15 Jan. 2024 represented a value of  $35.71\text{ }^\circ\text{C}$ . The value of the COP represents number 2.6 by the heat carrier

Table 2 Values of the thermal energy and electric consumption

Day of January	7	8	9	10	11	12	13	14	15
Floor [kWh]	18	20	21	26	27	24	25	23	12
Ceiling [kWh]	19	22	23	28	30	27	27	26	14
Wall [kWh]	17	29	20	25	26	23	24	22	12
ASHP [kWh]	17	25	26	34	35	25	28	24	13

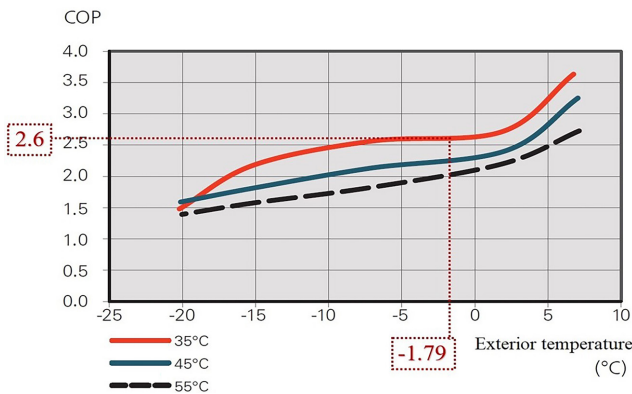


Fig. 9 Performance number heat pump F 2040-6 at different output temperatures of the heat-carrying working substance [20, 24]

temperature of 35 °C and exterior temperature  $-1.79$  °C (Fig. 9). We determined the average values of the exterior air temperature and the values of the COP for the heat-carrying working substance 35 and 45 °C of the individually day (Table 3).

Table 2 and Fig. 8 show the measured values of the thermal energy consumption by the radiant systems and electric consumption by the ASHP. We calculated the SPF values by the using Eq. (1). Fig. 10 shows the calculated SPF values for individual days displays by blue columns. The orange points show the average exterior temperature values of individual days. We see that during the four days from 8 Jan. until 11 Jan. 2024, which have negative

Table 3 Values of the SPF and COP for individually tested days

Day of January	7	8	9	10	11	12	13	14	15
Average Exterior temp.	0.5	-4.2	-5	-4.2	-2.6	0.2	-0.5	0.4	0.0
SPF	3.2	2.4	2.5	2.3	2.4	3.0	2.7	3.0	2.9
COP (35 °C)	2.7	2.6	2.6	2.6	2.6	2.6	2.6	2.7	2.6
COP (45 °C)	2.3	2.2	2.2	2.2	2.2	2.3	2.3	2.3	2.3

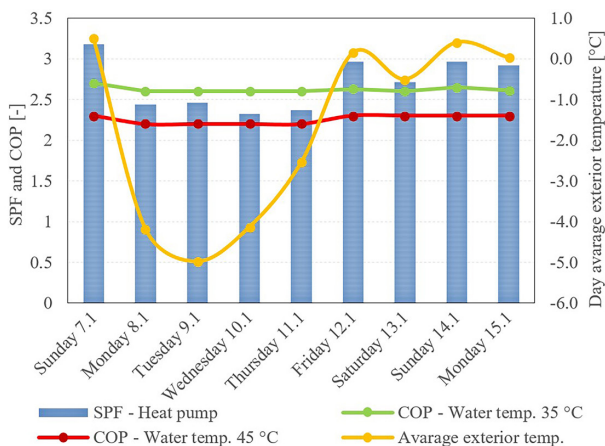


Fig. 10 The SPF and COP of the ASHP during measured period

values of the average outdoor temperature, the SPF values are also lower (Table 3).

The SPF of the ASHP was calculated from 7 Jan. 2024 to 10 Jan. 2024 at 9:00 a.m., resulting in an SPF value of 2.58 and COP of 2.6 by the average exterior temperature  $-3.32$  °C. and by the average heat carrier substance temperature of  $32.56$  °C. From 10 Jan. 2024 at 9:00 a.m. to 15 Jan. 2024 until 12:30 p.m., the SPF was 2.70 and COP of 2.6 by the average exterior temperature  $-0.79$  °C. and by the average heat carrier substance temperature of  $37.77$  °C.

During the measured period from 7 Jan. 2024 to 15 Jan. 2024, the SPF was 2.64. The determination of the COP value was based on the curve representing the heat transfer substance of 35 °C. The SPF values calculated are displayed as blue bars in Fig. 10.

### 5 Conclusion

ASHP as a heat source in cooperation with the SMO S40 control unit in connection with large-area low-temperature radiant systems, work in heating mode effectively. ASHP uses environmental energy (in this case air) to produce heat, what reduce consumption of the traditional fossil fuels, as for example natural gas.

To assess the efficiency of ASHP operation with radiant systems in the heating mode, we calculated the SPF values. The SPF values were calculated is the ratio of the heat supplied by the ASHP (heat energy consumption by the radiant systems) the total energy consumed by the compressor and other circulation devices (electric consumption) during the testing period from 7 Jan. 2024 to 15 Jan. 2024 the total energy consumed by the compressor and other circulation devices. It should be noted that the calculated SPF value is more reliable (real existing building with heat pump and radiant systems, real operation of the system with equithermal regulation) compared to the COP value declared by the manufacturer (laboratory conditions of operation of the heat pump at a constant heat-carrying working substance temperature).

Our main goal was calculated the SPF value of the ASHP in cooperation with radiant systems in heating mode for the testing period from 5 Jan. 2024 to 15 Jan. 2024 and compare with declared COP value by the manufacturer. The calculated SPF value during the test period from 7 Jan. 2024 to 15 Jan. 2024 was 2.64. During this tested period the average exterior temperature was  $-1.79$  °C and the average heat carrier substance temperature was  $35.71$  °C which corresponds to the COP value of 2.6 declared by the manufacturer. The SPF value is dependent on the outside temperature and the temperature of the heat carrier (Fig. 10). The tested system with ASHP was

controlled by equithermal regulation, which means that when the exterior temperature changes, ASHP ensured the water temperature according to the equithermal curve.

The calculated SPF value of 2.66 during the tested period from 7 Jan. 2024 to 15 Jan. 2024 corresponds to the value of 2.6 declared by the manufacturer.

## References

- [1] Junasová, B., Krajčík, M., Šikula, O., Arici, M., Šimko, M. "Adapting the construction of radiant heating and cooling systems for building retrofit", *Energy and Buildings*, 268, 112228, 2022. <https://doi.org/10.1016/j.enbuild.2022.112228>
- [2] Krajčík, M., Arici, M., Šikula, O., Šimko, M. "Review of water-based wall systems: Heating, cooling, and thermal barriers", *Energy and Buildings*, 253, 111476, 2021. <https://doi.org/10.1016/j.enbuild.2021.111476>
- [3] Maatouk, C., Zoughaib, A., Clodic, D. "New methodology of characterization of seasonal performance factor of an air-to-water heat pump", In: *International Refrigeration and Air Conditioning*, Purdue, Lafayette, Indiana, USA, 2010, 2279, 19648486.
- [4] Madonna, F., Bazzocchi, F. "Annual performances of reversible air-to-water heat pumps in small residential buildings", *Energy and Buildings*, 65, pp. 299–309, 2013. <https://doi.org/10.1016/j.enbuild.2013.06.016>
- [5] Bin, H., Wang, R. Z., Biao, X., Lin, H., Wei, Z., Shihang, Z. "Performance evaluation of different heating terminals used in air source heat pump system", *International Journal of Refrigeration*, 98, pp. 274–282, 2019. <https://doi.org/10.1016/j.ijrefrig.2018.10.014>
- [6] Dongellini, M., Naldi, C., Morini, G. L. "Seasonal performance evaluation of electric air-to-water heat pump systems", *Applied Thermal Engineering*, 90, pp. 1072–1081, 2015. <https://doi.org/10.1016/j.applthermaleng.2015.03.026>
- [7] Shao, S., Zhang, H., Fan, X., You, S., Wang, Y. "Thermodynamic and economic analysis of the air source heat pump system with direct-condensation radiant heating panel", *Energy*, 225, 120195, 2021. <https://doi.org/10.1016/j.energy.2021.120195>
- [8] Verhelst, C., Degrauwe, D., Logist, F., Van Impe, J., Helsen, L. "Multi-objective optimal control of an air-to-water heat pump for residential heating", *Building Simulation*, 5, pp. 281–291, 2012. <https://doi.org/10.1007/s12273-012-0061-z>
- [9] Zhang, L., Dong, J., Deng, S., Yan, S. "An experimental study on the starting characteristics of an improved radiant-convective air source heat pump system", *Energy and Buildings*, 226, 110384, 2020. <https://doi.org/10.1016/j.enbuild.2020.110384>
- [10] Liu, D., Li, G., Wu, X., Wang, J., Hu, A., Yan, Q., Yang, X., Yhou, H. "Comparative analysis of heating characteristics of convective-radiant systems using various terminal air source heat pumps", *Energy and Buildings*, 301, 113701, 2023. <https://doi.org/10.1016/j.enbuild.2023.113701>
- [11] Zhao, M., Kang, W., Gu, Z. "Performance comparison of capillary mat radiant and floor radiant heating systems assisted by an air source heat pump in a residential building", *Indoor and Built Environment*, 26(9), pp. 1292–1304, 2017. <https://doi.org/10.1177/1420326X16674517>
- [12] Babiak, J., Olesen, B. W., Petráš, D. "Low temperature heating and high temperature cooling", *REHVA Federation of European Heating, Ventilation and Air Conditioning Associations*, 2007. ISBN 2-9600468-6-2
- [13] Kassai, M. "Heat pump heating system development of educational building based on energy, economical and environmental impacts", *Periodica Polytechnica Mechanical Engineering*, 63(3), pp. 207–213, 2019. <https://doi.org/10.3311/PPme.13872>
- [14] Komlós, F., Fodor, Z., Kapros, Z., Vajda, J., Vaszil, L. "Hőszivattyús rendszerek", (English title) *Jordán Print Nyomdaipari Bt., Komlós Ferenc*, 2009. ISBN 978-963-06-7574-1 (in Hungarian) [online] Available at: <https://www.antikvarium.hu/konyv/komlos-ferenc-fodor-zoltan-hoszivattyus-rendszerek-1020439-0> [Accessed: 12 October 2024]
- [15] Garbai, L., Méhes, S. "System theory models of different types of heat pumps", presented at *Proceedings of the 2nd IASME / WSEAS International Conference on Energy & Environment (EE'07)*, Portoroz, Slovenia, May, 15–17, 2007. [online] Available at: [https://www.researchgate.net/publication/242067050\\_System\\_Theory\\_Models\\_of\\_Different\\_Types\\_of\\_Heat\\_Pumps](https://www.researchgate.net/publication/242067050_System_Theory_Models_of_Different_Types_of_Heat_Pumps) [Accessed: 12 October 2024]
- [16] Kwon, Y., Bae, S., Nam, Y., Yun, R., Park, C. Y., Lee, H. "Comparative analysis of system performance for water, ground and air source heat pump system using the dynamic energy simulation", *Journal of the Korean Solar Energy Society*, 41(4), pp. 1–12, 2021. <https://doi.org/10.7836/kses.2021.41.4.001>
- [17] Çakır, U., Çomaklı, K., Çomaklı, Ö., Karşlı, S. "An experimental exergetic comparison of four different heat pump systems working at same conditions: As air to air, air to water, water to water and water to air", *Energy*, 58, pp. 210–219, 2013. <https://doi.org/10.1016/j.energy.2013.06.014>
- [18] Chesser, M., Lyons, P., O'Reilly, P., Carroll, P. "Air source heat pump in-situ performance", *Energy and Buildings*, 251, 111365, 2021. <https://doi.org/10.1016/j.enbuild.2021.111365>

- [19] O'Hegarty, R., Kinnane, O., Lennon, D., Colclough, S. "Air-to-water heat pumps: Review and analysis of the performance gap between in-use and product rated performance", *Renewable and Sustainable Energy Reviews*, 155, 111887, 2022. <https://doi.org/10.1016/j.rser.2021.111887>
- [20] NIBE "Installation manual", [online] Available at: <https://www.nibe.eu/sk/sk/produkty/tepelne-cerpadla/tepelne-cerpadla-vzduch-voda/f2040> [Accessed: 05 March 2024]
- [21] CEN "EN 14825:2022 Air conditioners, liquid chilling packages and heat pumps, with electrically driven compressors, for space heating and cooling, commercial and process cooling. Testing and rating at part load conditions and calculation of seasonal performance", CEN, Brussel, Belgium, 2022. [online] Available at: [https://standards.iteh.ai/catalog/standards/cen/9fcc3835-2b65-478e-920e-3f3bacb6d2c5/en-14825-2022?srsId=AfmBOoqLmqxk6Li4mq5KvjL7tNMC1Z\\_YvP9C1\\_qrEPDJHE\\_uLBkQiyof](https://standards.iteh.ai/catalog/standards/cen/9fcc3835-2b65-478e-920e-3f3bacb6d2c5/en-14825-2022?srsId=AfmBOoqLmqxk6Li4mq5KvjL7tNMC1Z_YvP9C1_qrEPDJHE_uLBkQiyof) [Accessed: 12 October 2024]
- [22] Petráš, D., Lulkovičová, O., Takács, J., Fűri, B. "Renewable energy sources for low-temperature systems", Jaga Group, s. r. o., 2009. ISBN 978-80-8076-075-5. [online] Available at: <https://www.jagastore.sk/tzb/obnovitelne-zdroje-energie-pre-nizkoteplotne-systemy/> [Accessed: 12 October 2024]
- [23] CEN "EN 15316-4-2:2017 Energy performance of buildings – Method for calculation of system energy requirements and system efficiencies – Part 4–2: Space heating generation systems, heat pump systems", CEN, Brussel, Belgium, 2017.
- [24] CEN "EN 14511-1:2022 Air conditioners, liquid chilling packages and heat pumps for space heating and cooling and process chillers, with electrically driven compressors – Part 1: Terms and definitions", CEN, Brussel, Belgium, 2022.